Confined Synthesis of Carbon Nitride in a Layered Host Matrix with Unprecedented Solid-State Quantum Yield and Stability

Wendi Liu, Simin Xu, Shanyue Guan, Ruizheng Liang,* Min Wei,* David G. Evans, and Xue Duan

Fluorescent carbon nanomaterials have drawn tremendous attention for their intriguing optical performances, but their employment in solid-state luminescent devices is rather limited as a result of aggregation-induced photoluminescence quenching. Herein, ultrathin carbon nitride (CN) is synthesized within the 2D confined region of layered double hydroxide (LDH) via triggering the interlayer condensation reaction of citric acid and urea. The resulting CN/LDH phosphor emits strong cyan light under UV-light irradiation with an absolute solid-state quantum yield (SSQY) of 95.9 ± 2.2%, which is, to the best of our knowledge, the highest value of carbon-based fluorescent materials ever reported. Furthermore, it exhibits a strong luminescence stability toward temperature, environmental pH, and photocorrosion. Both experimental studies and theoretical calculations reveal that the host–guest interactions between the rigid LDH matrix and interlayer carbon nitride give the predominant contribution to the unprecedented SSQY and stability. In addition, prospective applications of the CN/LDH material are demonstrated in both white light-emitting diodes and upconversion fluorescence imaging of cancer cells.

Fluorescent carbon nanomaterials (such as carbon nanotubes, fullerenes, graphene derivatives, nanodiamonds) possess intriguing optical properties owing to their manifold structure, morphology, and functionalization.[1–3] Especially in recent years, carbon dots (CDs) and graphene quantum dots (GQDs) have drawn tremendous attention for their high aqueous solubility, facile preparation, and low toxicity; and prospective applications have been explored in bioimaging, photocatalysis, photovoltaic, and optoelectronic devices.[4–7] Great efforts have been made to promote the photoluminescence quantum yield (PLQY) of CDs and GQDs, which is a crucial factor in practical applications.[8–12] However, previous studies on nanocarbon fluorescent materials are mainly focused on aqueous or colloid systems; solid-state quantum yield (SSQY) decreases sharply

as a result of aggregation-induced PL quenching, which restricts their employment in solid state devices (e.g., light-emitting diodes (LEDs), optoelectronic devices).[13–15] Meanwhile, the fluorescent intensity is highly susceptible to external environments such as temperature or pH value, which seriously affects the implementation of practical illumination.[16–20] Therefore, how to attain carbon materials based phosphors with excellent SSQY and stability simultaneously via material design and synthesis exploration is of scientific and technological importance, and remains a challenge.

Graphitic carbon nitride (g-C_3N_4), with appropriate electronic band structure, has been demonstrated as excellent photocatalysts for water splitting, CO_2 reduction, pollutant degradation, etc.[21–24] Many endeavors on its nanoarchitecture design and energy level modification have been made, aiming for enhanced photo/electrical performances.[25–28] In contrast to graphene, g-C_3N_4 possesses inherent fluorescence originating from C−N conjugated structure, making it good candidate for optical applications.[29–31] However, bulk g-C_3N_4 synthesized by traditional thermal condensation method normally gives rather low SSQY (≈5%).[32,33] In order to improve the fluorescent efficiency, several preparative protocols (e.g., ultrasound or acid treatment) have been explored to cleave bulk g-C_3N_4 to ultrathin nanosheets or ultrasmall nanodots in aqueous environment, with largely increased PLQY.[33–40] But the solid state luminescent applications (e.g., light emitting devices) still cannot be guaranteed on account of subsequent assembly-induced or aggregation-induced fluorescence quenching. Thus, how to overcome this contradiction is a key point. If ultrathin carbon nitride nanosheets can be in situ synthesized within a solid 2D host matrix through bottom-up route, the aggregation will be eliminated and a photoluminescence material with higher SSQY would be obtained; moreover, by choosing host material with appropriate bandgap, the host–guest interaction would further enhance the SSQY and stability.

Layered double hydroxides (LDHs) are a typical class of 2D inorganic materials with positively charged host matrix and exchangeable interlayer anions, which provides an ideal microenvironment for in situ interlayer synthesis reaction.[41–43]

W. Liu, Dr. S. Xu, Dr. S. Guan, Dr. R. Liang, Prof. M. Wei,
Prof. D. G. Evans, Prof. X. Duan
State Key Laboratory of Chemical Resource Engineering
Beijing Advanced Innovation Center for Soft Matter
Science and Engineering
Beijing University of Chemical Technology
Beijing 100029, China
E-mail: liangruizheng2000@163.com; weimin@mail.buct.edu.cn

**ADVANCED
SCIENCE NEWS**
www.advancedsciencenews.com

**ADVANCED
MATERIALS**
www.advmat.de

Herein, highly emissive ultrathin carbon nitride was synthesized within the 2D confined region of MgAl-LDH via triggering the interlayer condensation of urea and citric acid (CA). The resulting carbon nitride intercalated in LDH (CN/LDH) emits strong cyan light upon UV light irradiation with a SSQY of 95.9 ± 2.2%, which is, to the best of our knowledge, the highest value of fluorescent carbon materials ever reported.[15,34,37,44–48] Furthermore, the strong luminescence of CN/LDH is extremely inert to external stimulus including temperature and environmental pH, and its stability toward photobleaching is rather satisfactory. Although a great progress on the preparation of solid-state fluorescent materials by means of solid matrix dispersion has been reported,[48,49] carbon-based phosphor with such a high SSQY and stability simultaneously is rarely documented. Both experimental studies and theoretical calculation reveal that the host–guest interactions between rigid LDH matrix and interlayer carbon nitride give contribution to the unprecedented SSQY and stability. In addition, prospective applications of this CN/LDH material were demonstrated both in white light emitting diodes (WLEDs) and upconversion fluorescence imaging of cells.

The in situ systhesis of CN/LDH material is displayed in **Figure 1**a: citric acid was first intercalated into MgAl-LDH gallery (CA/LDH) through a separate nucleation and aging steps method reported by our group,[50] which showed a nanoplatelet morphology with a particle size of ≈60 nm (Figure 1b). Subsequently, the CA/LDH was thoroughly dispersed in a urea aqueous solution through supersonic treatment, followed by heating in a 650 W microwave reactor for 5 min for the interlayer reaction. The resulting yellow powdered product inherits the sheet-like morphology of CA/LDH precursor, with a slight increase in particle size (Figure 1c). The X-ray diffraction (XRD) pattern of CA/LDH (Figure S1a, Supporting Information) can be indexed to a rhombohedral LDH phase with an interlayer distance (d_{003}) of 1.17 nm, in accordance with the summation of an LDH monolayer thickness and the size of CA molecule. After the microwave-assisted interlayer reaction, the XRD pattern of the product (Figure S1a, Supporting Information) shows the (002) reflection of carbon nitride phase,[21,51] suggesting the formation of carbon nitride species in the interlayer region (CN/LDH). The small angle XRD pattern of CN/LDH exhibits a slight shift of (003) reflection to a low 2θ value (Figure S1b, Supporting Information), indicating an expansion of interlayer space after the reaction (from 1.17 to 1.21 nm). The formation of carbon nitride structure is further characterized by X-ray photoelectron spectroscopy (XPS) spectra (Figure S2, Supporting Information). The C1s spectrum shows three carbon species: 288.7 eV for N−C=N, 286.3 eV for C−N and 284.5 eV for C=C. The N1s spectrum can be deconvoluted into three peaks, including 398.8 eV for C−N=C, 400.0 eV
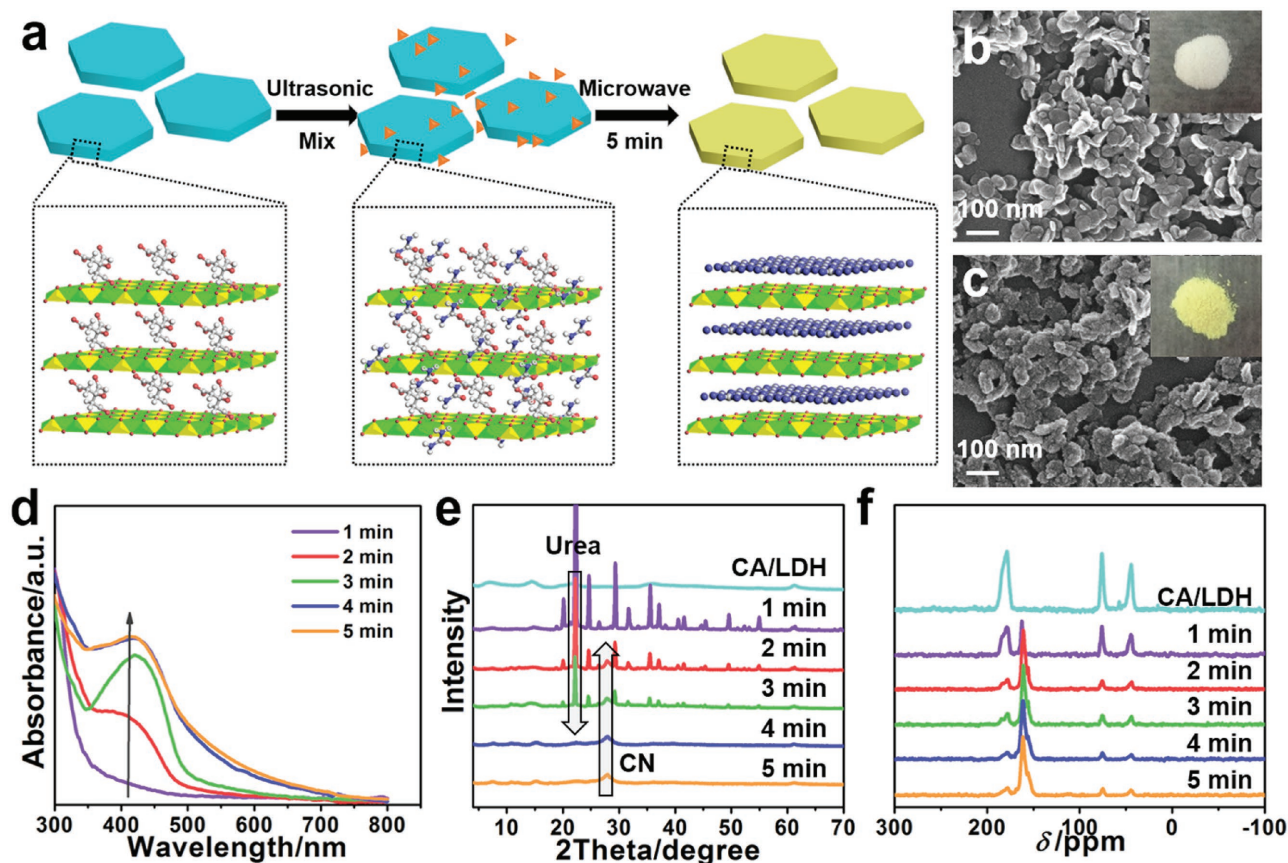

Figure 1. a) Schematic representation for the synthesis of CN/LDH composite. SEM images of b) CA/LDH and c) CN/LDH; the insets show the photographs of CA/LDH and CN/LDH under daylight. d) UV–vis absorption spectra, e) XRD patterns, and f) ^{13}C MAS NMR spectra of CA/LDH and CN/LDH prepared with different reaction times (1–5 min).

for N—(C)₃ and 401.7 eV for N—H, respectively. The organic elemental analysis gives a N/C molar ratio of 1.08 for the CN/LDH sample (Table S1, Supporting Information), smaller than the theoretical carbon nitride structure (1.33). The extra carbon atoms might be due to the formation of unsaturated C=C as shown in C1s XPS spectra.

The UV–vis spectra, XRD patterns, and solid-state nuclear magnetic resonance (NMR) spectra of CN/LDH samples with different synthesis time were performed to monitor the reaction process. The UV–vis spectra in Figure 1d show that the absorption band at ≈410 nm enhances progressively with the increase of reaction time from 1 to 5 min, indicating the gradual formation of carbon nitride structure.[52,53] The absorption edge displays a slight red shift relative to typical carbon nitride, possibly due to the simultaneous formation of conjugated C=C bond as observed in the XPS spectra (Figure S2a, Supporting Information). In the case of XRD patterns (Figure 1e), the reflections corresponding to urea vanish over reaction time, and the (002) diffraction peak of carbon nitride at 2θ 27.8° appears at 2 min and increases afterward.[54] Solid-state ^{13}C NMR spectra show gradually decreased characteristic peaks of CA (Figure 1f; Figure S3, Supporting Information), accompanied with the appearance of new peaks due to sp^2 C. Notably, two peaks at 168 and 154 ppm are observed, which can be ascribed to $CN_2(NH_x)$ and CN_3 group in carbon nitride, respectively.[55,56] Moreover, the peak at $\delta = 10.2$ ppm in ^{27}Al NMR spectra suggests that aluminum is principally located in an octahedral environment (Figure S4, Supporting Information), indicating the maintenance of LDH structure.[57] The results above confirm the formation of carbon nitride via the microwave-induced interlayer reaction, which is the source of photoluminescence.

To further investigate the structure of synthesized material, LDH host matrix was etched with hydrochloric acid to release the interlayer species. After a dialysis and centrifugation operation, yellow powdered product was obtained and denoted as R-CN. Strong (100) and (002) reflection of carbon nitride phase at 13.7° and 27.8° are observed in the XRD pattern, with tiny unknown impure phases (Figure S5a, Supporting Information). The Fourier transform infrared spectroscopy (FT-IR) spectrum shows characteristic band at 800 cm^{-1} (Figure S5b, Supporting Information) due to the out-of-plane bending vibration of conjugated carbon nitride, and the bands at 1400–1650 cm^{-1} are assigned to stretching vibration modes of C—N ring system.[54] Transmission electron microscopy (TEM) image (Figure S6a,b, Supporting Information) shows a lamellate morphology of R-CN with a diameter of ≈20 nm; the lattice fringe of 0.32 nm can be identified in the high resolution TEM image (Figure S6c, Supporting Information), corresponding to the (002) plane of carbon nitride. Besides, the thickness of R-CN nanosheets is determined to be ≈0.74 nm by tapping mode atomic force microscopy measurements (Figure S7, Supporting Information), which is in accordance with the interlayer gallery of CN/LDH based on XRD pattern (subtracting the thickness of LDH monolayer, 0.48 nm, from the d_{003} value).

The light yellow CN/LDH powdered sample gives strong cyan fluorescnce under UV light irradiation. Solid-state photoluminescence measurements show that the emission maxima of CN/LDH is 495 nm with an optimal excitation wavelength of 380 nm (**Figure 2**a). In 3D fluorescence spectra (Figure 2b), only

one luminous center is observed without excitation-dependent PL property, indicating the purity of fluorophore. Interestingly, the absolute SSQY of CN/LDH is measured to be 95.9 ± 2.2% at room temperature in ambient atmosphere, and the solid-state PL decay is monoexponential with a lifetime of 14.01 ± 0.18 ns (Figure 2c; Table S2, Supporting Information). The SSQY value is unprecedentedly high compared with carbon nitrides, carbon dots, and graphene quantum dots materials ever reported. Different from the fluorescent dyes, semiconductor quantum dots, and carbon dots which are normally erratic toward external stimulations such as temperature and pH, the PL performance of CN/LDH is rather stable in various environments. As shown in Figure 2d, only a slight decrease in the PL intensity is observed when the temperature drastically increases from 93 to 393 K. Similarly, the fluorescence decays at various temperatures do not show obvious difference (Figure 2e; Table S3, Supporting Information). After a supersonic treatment, the CN/LDH sample can be uniformly dispersed in water with an equivalent hydrodynamic diameter of ≈80 nm (Figure S8a, Supporting Information), and the colloid suspension emits strong light under UV light irradiation with an absolute PLQY of 80.5%. The emission wavelength remains almost constant upon variable excitation wavelength (Figure S8b, Supporting Information). The PL intensity is very stable within pH value 5.0–9.0 (Figure 2f), and decreases in a strong alkaline environment (pH = 11.0). The stability of CN/LDH sample against photobleaching was tested, whose PL intensity remained almost unchanged either upon irradiation at 365 nm for 6 h or at a high temperature of 373 K for 2 h (Figure 2g; Figure S9, Supporting Information). By contrast, the bare R-CN sample shows an inferior stability: 15% and 4% losses in PL intensity are detected under the same conditions. Most importantly, the CN/LDH sample exhibits effective upconversion photoluminescence (UCPL) performance. Under irradiation by a 800 nm femtosecond pulsed laser with various power, the CN/LDH phosphor gives an identical emission peak at 490 nm, close to the fluorescence position excited by UV light (Figure 2h). The quadratic dependence between PL intensity and laser power confirms that the present UCPL is a two-photon excitation process (Figure 2i).

To further understand the key role of confined interlayer environment on the PL behavior of CN/LDH, two control samples are prepared: the first (C1) is synthesized by the microwave-assistant reaction of CA and urea without the LDH host matrix under the same reaction conditions; the second one (C2) is synthesized from carbonate-intercalated MgAl-LDH (CO_3^{2-}-LDH) with corresponding amount of CA and urea. The C1 sample shows undetectable emission under UV light while C2 sample emits relatively bright green light at 514 nm (**Figure 3**a), with the absolute SSQY values of 0.53% and 42.9%, respectively. The different PL properties between control samples and CN/LDH are due to the different structures as shown in XRD patterns (Figure 3b). For the synthesis of C1, a severe carbonization occurs with a large amount of nonfluorescent graphite phase. After the introduction of CO_3^{2-}-LDH in the reaction system, CA and urea undergo condensation reaction on the surface of LDH, promoting the growth of carbon nitride phase but with the formation of non-neglectable amorphous phase. In the case of CN/LDH preparation, CA molecules are located in LDH
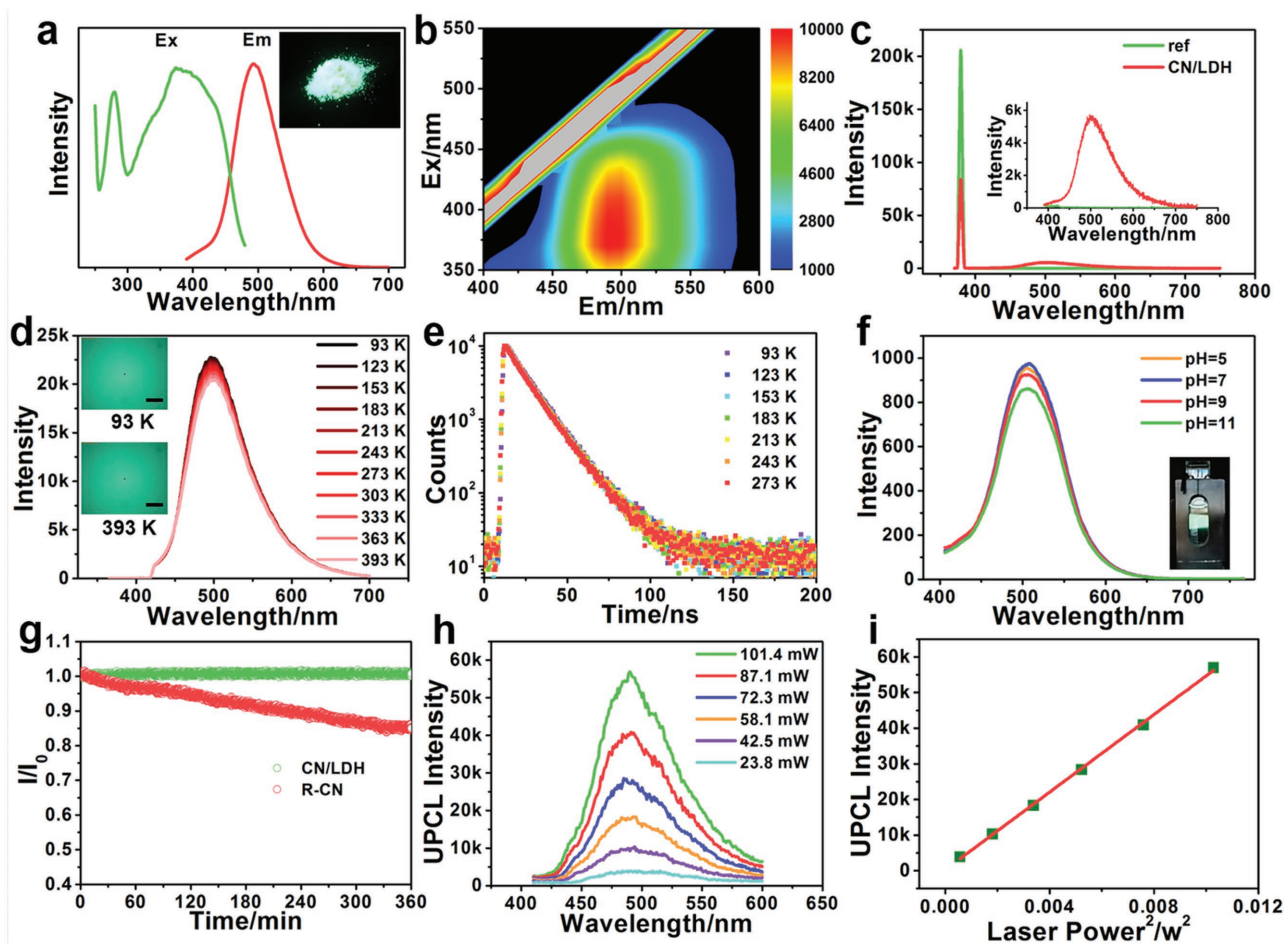
ADVANCED
SCIENCE NEWS
www.advancedsciencenews.com

ADVANCED
MATERIALS
www.advmat.de

Figure 2. a) Fluorescence excitation and emission spectra of CN/LDH (inset shows the photograph under UV light) and b) the corresponding 3D fluorescence spectra. c) Emission spectrum used for the absolute solid-state quantum yield determination of CN/LDH; the inset shows the amplified portion of the emission within 390–750 nm. d) In situ fluorescence spectra of CN/LDH in the temperature range 93–393 K by using a micro-spectro-photometer with a cryostat; the insets display fluorescent microscopy images at 93 and 393 K. e) Typical fluorescence decay curves of CN/LDH in the temperature range 93–273 K. f) PL spectra of CN/LDH in aqueous solution with pH value ranging in 5–11. g) Photostability test over CN/LDH and R-CN upon irradiation by UV light (365 nm) for 6 h. h) UCPL spectra of CN/LDH with variable power of excitation laser. i) UCPL intensity as a function of square of laser power (800 nm femtosecond pulsed laser was applied throughout).

interlamination, and the reaction takes place in the interlayer region with carbon nitride phase as the only product. This is further proved by the solid-state ^{13}C NMR spectra, in which C2 sample and CN/LDH show similar $CN_2(NH_x)$ and CN_3 groups at 168 and 154 ppm while C1 sample displays the presence of a large amount of C=C bond without PL property (Figure 3c). The UV–vis spectra also reveal the different carbonization degree of the three samples (Figure 3d). We also synthesized two control samples without the addition of CA: C3 was prepared from pure urea under the same reaction conditions and C4 was prepared from urea and CO_3^{2-}-LDH similarly. These two samples show very weak fluorescence under UV light (Figure S10a, Supporting Information) and low SSQY (8.83% and 0.77%), indicating that CA plays an important role in the production of carbon nitride structure. The sample of C3 displays a rather weak XRD diffraction peak of carbon nitride with major proportion of impurity; while carbon nitride is hardly observed in the sample of C4 (Figure S10b, Supporting Information). This is further verified by the UV–vis spectra (Figure S10c, Supporting

Information). As demonstrated above, the bright fluorescence originates from the carbon nitride structure. Moreover, the variation in structure indicates the existence of LDH prevents the carbonization process and facilitates the growth of carbon nitride phase, which is especially strengthened in the confined LDH interlamination.

Several factors would contribute to the extremely high SSQY of CN/LDH sample. First, the confinement effect imposed by the host–guest interaction significantly inhibits the excited-electron-transfer and enhances the electron–hole recombination process.[58–60] In addition, LDHs host matrix serves as spacer to isolate the ultrathin carbon nitride species, which avoids aggregation induced fluorescence quenching. Finally, a covalent bonding between LDHs matrix and carbon nitride might occur, resulting in highly emissive species. The host–guest interaction on the fluorescent performance of CN/LDH was investigated. After removing the LDH matrix by acid etching, the excitation and emission peak of R-CN show a significant red shift (**Figure 4**a);

ADVANCED
SCIENCE NEWS
www.advancedsciencenews.com
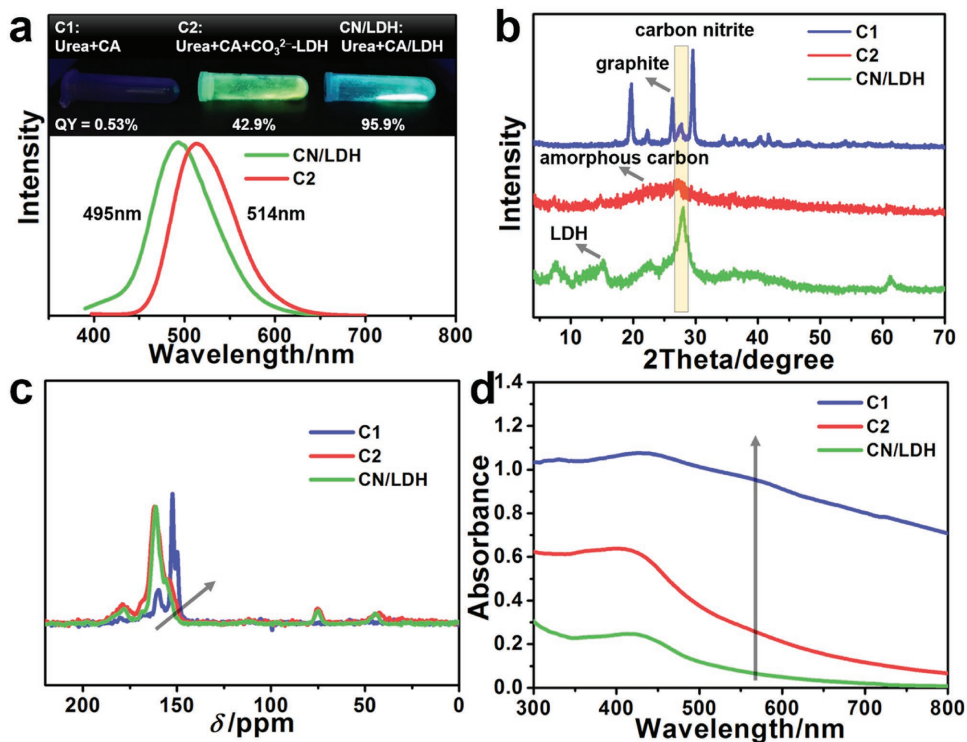
ADVANCED
MATERIALS
www.advmat.de

Figure 3. Characterizations of CN/LDH and two control samples (C1 and C2): a) fluorescence spectra and photographs under UV-light irradiation; b) XRD patterns; c) ^{13}C MAS NMR spectra; d) UV–vis absorption spectra.

the SSQY of R-CN declines sharply from 95.9% to 29.9%, as well as the fluorescence lifetime (from 14.01 to 11.56 ns) (Figure 4b). This indicates the vanishing of the confinement effect imposed by the host–guest interaction. The highest occupied molecular orbital (HOMO) and lowest unoccupied molecular orbital (LUMO) energy levels of R-CN are studied
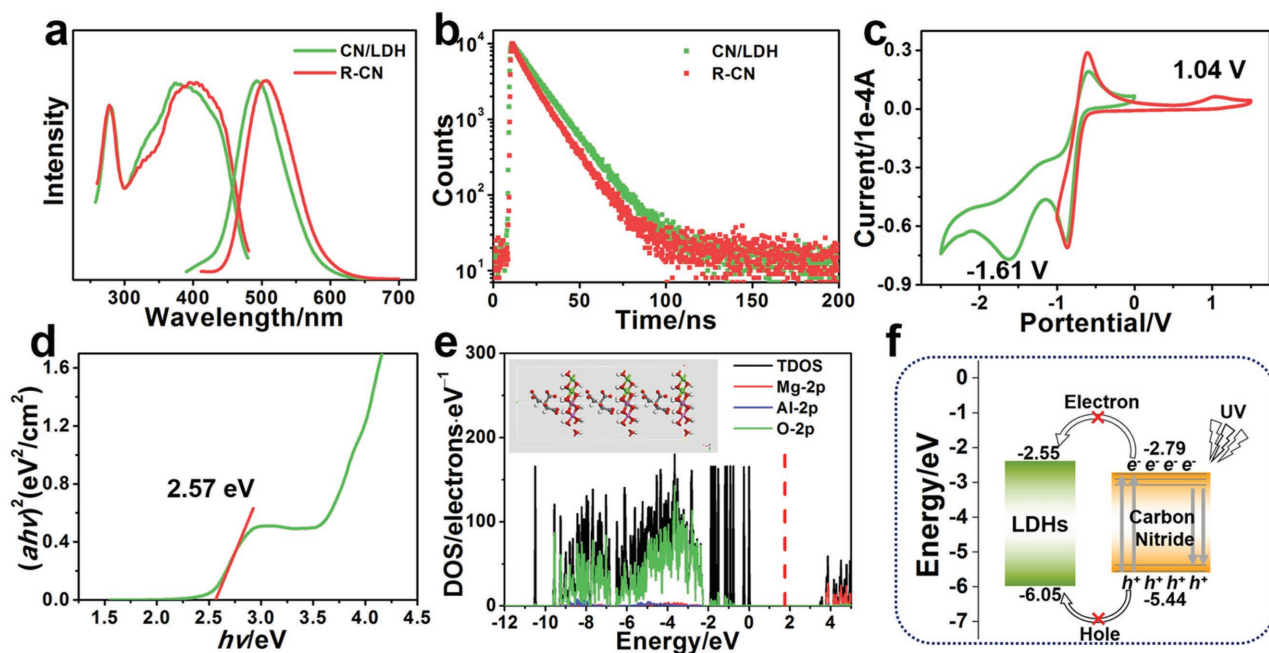

Figure 4. a) Fluorescence excitation and emission spectra of CN/LDH and R-CN. b) Typical fluorescence decay curves of these two samples. c) Cyclic voltammogram curves of R-CN: the positive scan (red line) and negative scan (green line). d) UV–vis absorption threshold of R-CN. e) Density of states for MgAl-LDH (inset shows the optimized geometry). f) Band edge placement of MgAl-LDH and R-CN.

**ADVANCED
SCIENCE NEWS**
www.advancedsciencenews.com

**ADVANCED
MATERIALS**
www.advmat.de

by cyclic voltammetry via a standard three electrode system, which are calculated to be −5.44 and −2.79 eV, respectively, based on the oxidation potential at 1.04 V and reduction potential at −1.61 V (Figure 4c, see detailed process in the Supporting Information). The bandgap of 2.65 eV is very close to the absorption edge of R-CN at 2.57 eV (Figure 4d). Density functional theory calculations are carried out to study the band edge placement of host matrix MgAl-LDH, and the HOMO and LUMO are calculated to be −6.05 and −2.55 eV with an energy gap of 3.50 eV (Figure 4e; Figure S11, Supporting Information). By comparing the band edge placement of R-CN and LDH, a mechanism for the enhanced SSQY in the CN/LDH system is proposed in Figure 4f. The LUMO energy of MgAl-LDH is higher than that of R-CN, while its HOMO energy is lower than that of R-CN. The photoinduced electron–hole pairs from intercalated carbon nitride are trapped in the energy well of LDH matrix, which effectively suppresses the excited transfer of carriers. Thus, the confinement effect facilitates the recombination of electrons and holes and promotes the efficiency of radiative transition, accounting for the extremely high SSQY of CN/LDH material.

Benefiting from its superior optical properties and stability, the CN/LDH material is particularly appropriate for application in solid state illumination and display. Through incorporation of the cyan CN/LDH and red emissive CdTe quantum dots absorbed on LDH (QD/LDH, Figure S12, Supporting Information) with various ratios, several phosphors with gradually changing color are obtained, as seen from the photographs under UV light (**Figure 5**a). The color coordinate CIE (Commission Internationale de l'Eclairage) measurements also demonstrate the luminescence color can be tuned from cyan (0.243, 0.441) to red (0.591, 0.274) by facilely changing the mass ratio
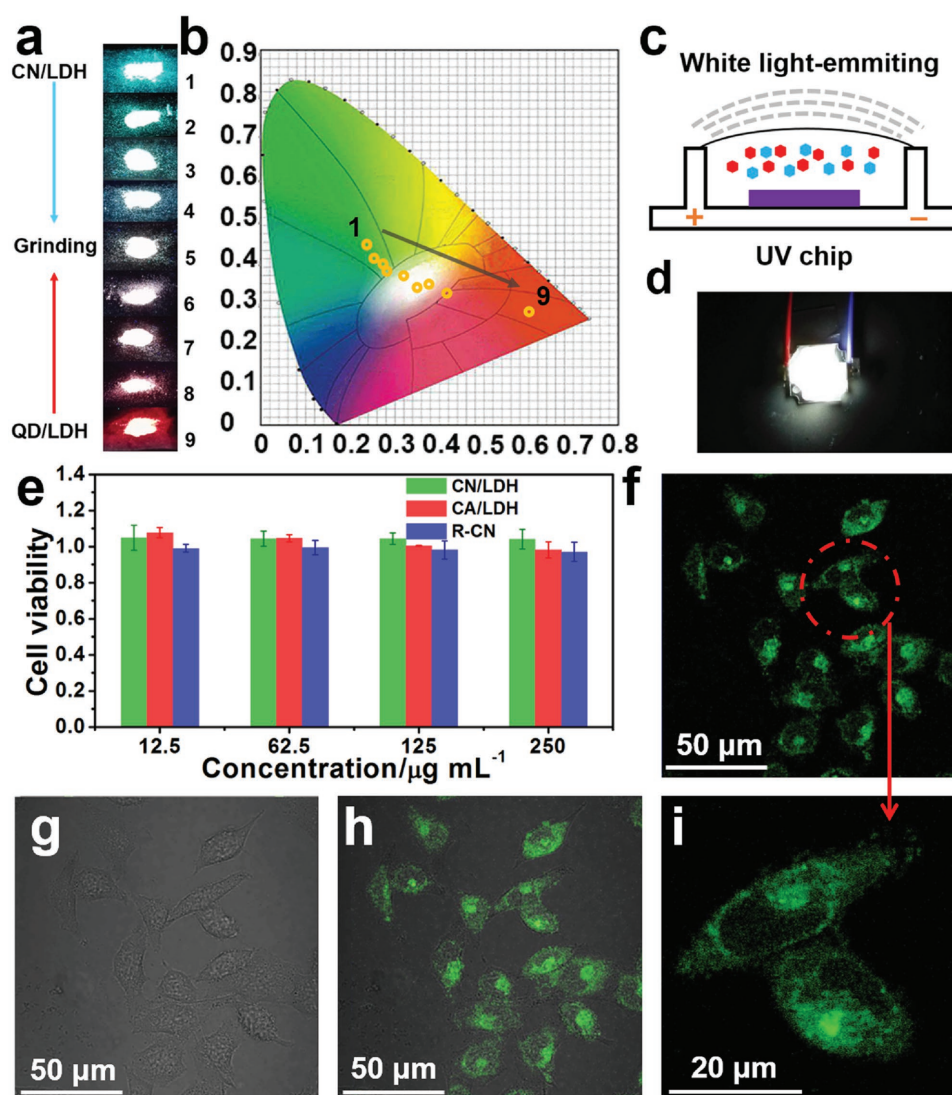

Figure 5. a) Photographs under UV light irradiation and b) CIE coordinates of mixed phosphors of CN/LDH and QD/LDH with various ratios: (1) CN/LDH, (2–8) CN/LDH:QD/LDH = 1:1, 1:2, 1:3, 1:6, 1:9, 1:15, 1:21, (9) QD/LDH. c) Schematic and d) photograph of the fabricated white LED. e) Cellular cytotoxicity assessment of CN/LDH, CA/LDH, and R-CN. f) Two-photon confocal fluorescence image, g) corresponding bright field image, and h) merged image of Hela cells incubated with CN/LDH under 800 nm laser excitation; i) fluorescence image with a high magnification.

**ADVANCED
SCIENCE NEWS**
www.advancedsciencenews.com

**ADVANCED
MATERIALS**
www.advmat.de

(Figure 5b; Table S4, Supporting Information). As the mass ratio of CN/LDH and QD/LDH is controlled as 1:9, the complex phosphor exhibits white light emission with color coordinate at (0.339, 0.334), very close to the pure white light (0.333, 0.333). A WLED based on this phosphor (CN/LDH:QD/LDH = 1:9) was further fabricated by mixing with polyvinyl alcohol and then coating on a commercial UV chip (Figure 5c,d). The device emits bright white light with the color rendering index and correlated color temperature of 92 and 4712 K, respectively, and the luminous efficiency is 5.6 lm W^{-1} (Figure S13, Supporting Information). This WLED shows a stable emission for 10 h without obvious intensity loss (Figure S14, Supporting Information), demonstrating CN/LDH can serve as a promising candidate in white-light optoelectronic devices. The study on white light emitting diodes through incorporation with Cd-based nanocrystals is a primary exploration, and related work on modulating emissive wavelength is in progress in our lab. In addition, its potential application as two-photon bioimaging agent was also explored. The cytotoxicity was evaluated by studying the viability of HeLa cells incubated with various concentrations of CA/LDH, CN/LDH, and R-CN for 24 h using the standard methyl thiazolyl tetrazolium method. The results show above 97% cell viabilities for all these three samples with concentration ranging from 12.5 to 250 μg mL^{-1}, indicating a satisfactory biocompatibility and nontoxicity (Figure 5e). After incubating Hela cells with CN/LDH for 4 h, a clear two-photon excitation confocal image is obtained by using a 800 nm single pulse laser (Figure 5f), and the bright field and merged images are shown in Figure 5g,h. In the cell image with a higher magnification (Figure 5i), the fluorescent signal is observed mainly in cytoplasm region, indicating an endocytosis of CN/LDH into HeLa cells.

In summary, layered carbon nitride was synthesized in 2D confined region of LDHs by microwave-induced condensation reaction of CA and urea. The resulting CN/LDH composite phosphor emits bright cyan light under UV light with an ultra-high SSQY of 95.9 ± 2.2%, which is the highest value among carbon dots, graphene quantum dots, and carbon nitrides based phosphors. This superior property is due to the inhibition on carbonization process and the formation of carbon nitride structure in the confined reaction; furthermore, the promotion toward photoexcited electron–hole recombination based on the host–guest electronic structure gives a predominant contribution. In addition, the CN/LDH phosphor exhibits strong stability against external stimulus (photo, heat, pH), which guarantees its prospective applications in WLED and upconversion cell imaging.

Supporting Information

Supporting Information is available online from the Wiley Online Library or from the author.

Acknowledgements

Conflict of Interest

The authors declare no conflict of interest.

Keywords

[1]   F. R. Baptista, S. A. Belhout, S. Giordani, S. J. Quinn, *Chem. Soc. Rev.* **2015**, *44*, 4433.
[2]   V. Georgakilas, J. A. Perman, J. Tucek, R. Zboril, *Chem. Rev.* **2015**, *115*, 4744.
[3]   O. Kozák, M. Sudolská, G. Pramanik, P. Cígler, M. Otyepka, R. Zbořil, *Chem. Mater.* **2016**, *28*, 4085.
[4]   S. N. Baker, G. A. Baker, *Angew. Chem., Int. Ed.* **2010**, *49*, 6726.
[5]   H. Li, Z. Kang, Y. Liu, S.-T. Lee, *J. Mater. Chem.* **2012**, *22*, 24230.
[6]   C. Ding, A. Zhu, Y. Tian, *Acc. Chem. Res.* **2014**, *47*, 20.
[7]   X. T. Zheng, A. Ananthanarayanan, K. Q. Luo, P. Chen, *Small* **2015**, *11*, 1620.
[8]   Y. Dong, H. Pang, H. B. Yang, C. Guo, J. Shao, Y. Chi, C. M. Li, T. Yu, *Angew. Chem., Int. Ed.* **2013**, *52*, 7800.
[9]   M. Zheng, S. Liu, J. Li, D. Qu, H. Zhao, X. Guan, X. Hu, Z. Xie, X. Jing, Z. Sun, *Adv. Mater.* **2014**, *26*, 3554.
[10] J. Hou, W. Wang, T. Zhou, B. Wang, H. Li, L. Ding, *Nanoscale* **2016**, *8*, 11185.
[11] S. Qu, D. Zhou, D. Li, W. Ji, P. Jing, D. Han, L. Liu, H. Zeng, D. Shen, *Adv. Mater.* **2016**, *28*, 3516.
[12] Y. Zhang, X. Liu, Y. Fan, X. Guo, L. Zhou, Y. Lv, J. Lin, *Nanoscale* **2016**, *8*, 15281.
[13] S. Qu, X. Wang, Q. Lu, X. Liu, L. Wang, *Angew. Chem., Int. Ed.* **2012**, *51*, 12215.
[14] S. Zhu, Q. Meng, L. Wang, J. Zhang, Y. Song, H. Jin, K. Zhang, H. Sun, H. Wang, B. Yang, *Angew. Chem., Int. Ed.* **2013**, *52*, 3953.
[15] Y. Chen, M. Zheng, Y. Xiao, H. Dong, H. Zhang, J. Zhuang, H. Hu, B. Lei, Y. Liu, *Adv. Mater.* **2016**, *28*, 312.
[16] P. Yu, X. Wen, Y.-R. Toh, J. Tang, *J. Phys. Chem. C* **2012**, *116*, 25552.
[17] C. Wang, Z. Xu, H. Cheng, H. Lin, M. G. Humphrey, C. Zhang, *Carbon* **2015**, *82*, 87.
[18] B. Kong, A. Zhu, C. Ding, X. Zhao, B. Li, Y. Tian, *Adv. Mater.* **2012**, *24*, 5844.
[19] H. Nie, M. Li, Q. Li, S. Liang, Y. Tan, L. Sheng, W. Shi, S. X.-A. Zhang, *Chem. Mater.* **2014**, *26*, 3104.
[20] H. Wang, J. Di, Y. Sun, J. Fu, Z. Wei, H. Matsui, A. del, C. Alonso, S. Zhou, *Adv. Funct. Mater.* **2015**, *25*, 5537.
[21] X. Wang, K. Maeda, A. Thomas, K. Takanabe, G. Xin, J. M. Carlsson, K. Domen, M. Antonietti, *Nat. Mater.* **2009**, *8*, 76.
[22] S. Cao, J. Low, J. Yu, M. Jaroniec, *Adv. Mater.* **2015**, *27*, 2150.
[23] W. J. Ong, L. L. Tan, Y. H. Ng, S. T. Yong, S. P. Chai, *Chem. Rev.* **2016**, *116*, 7159.
[24] J. Liu, Y. Liu, N. Liu, Y. Han, X. Zhang, H. Huang, Y. Lifshitz, S.-T. Lee, J. Zhong, Z. Kang, *Science* **2015**, *347*, 970.
[25] Y. Zhang, T. Mori, J. Ye, M. Antonietti, *J. Am. Chem. Soc.* **2010**, *132*, 6294.

[26] Z. Zhou, J. Wang, J. Yu, Y. Shen, Y. Li, A. Liu, S. Liu, Y. Zhang, *J. Am. Chem. Soc.* **2015**, *137*, 2179.

[27] J. Ji, J. Wen, Y. Shen, Y. Lv, Y. Chen, S. Liu, H. Ma, Y. Zhang, *J. Am. Chem. Soc.* **2017**, *139*, 11698.

[28] J. Xu, T. J. Brenner, L. Chabanne, D. Neher, M. Antonietti, M. Shalom, *J. Am. Chem. Soc.* **2014**, *136*, 13486.

[29] Y. Zhang, Q. Pan, G. Chai, M. Liang, G. Dong, Q. Zhang, J. Qiu, *Sci. Rep.* **2013**, *3*, 1943.

[30] Y. Kang, Y. Yang, L. C. Yin, X. Kang, L. Wang, G. Liu, H. M. Cheng, *Adv. Mater.* **2016**, *28*, 6471.

[31] Z. Song, T. Lin, L. Lin, S. Lin, F. Fu, X. Wang, L. Guo, *Angew. Chem., Int. Ed.* **2016**, *55*, 2773.

[32] D. Das, S. L. Shinde, K. K. Nanda, *ACS Appl. Mater. Interfaces* **2016**, *8*, 2181.

[33] X. Zhang, X. Xie, H. Wang, J. Zhang, B. Pan, Y. Xie, *J. Am. Chem. Soc.* **2013**, *135*, 18.

[34] L. Chen, D. Huang, S. Ren, T. Dong, Y. Chi, G. Chen, *Nanoscale* **2013**, *5*, 225.

[35] X. Zhang, H. Wang, H. Wang, Q. Zhang, J. Xie, Y. Tian, J. Wang, Y. Xie, *Adv. Mater.* **2014**, *26*, 4438.

[36] Z. Zhou, Y. Shen, Y. Li, A. Liu, S. Liu, Y. Zhang, *ACS Nano* **2015**, *9*, 12480.

[37] Y. Zhao, R. Wei, X. Feng, L. Sun, P. Liu, Y. Su, L. Shi, *ACS Appl. Mater. Interfaces* **2016**, *8*, 21555.

[38] J. Wu, S. Yang, J. Li, Y. Yang, G. Wang, X. Bu, P. He, J. Sun, J. Yang, Y. Deng, G. Ding, X. Xie, *Adv. Opt. Mater.* **2016**, *4*, 2095.

[39] Q. Cui, J. Xu, X. Wang, L. Li, M. Antonietti, M. Shalom, *Angew. Chem., Int. Ed.* **2016**, *55*, 3672.

[40] M. Rong, Z. Cai, L. Xie, C. Lin, X. Song, F. Luo, Y. Wang, X. Chen, *Chem. Eur. J.* **2016**, *22*, 9387.

[41] Q. Wang, D. O'Hare, *Chem. Rev.* **2012**, *112*, 4124.

[42] J. Sun, H. Liu, X. Chen, D. G. Evans, W. Yang, X. Duan, *Adv. Mater.* **2013**, *25*, 1125.

[43] B. Li, Z. Gu, N. Kurniawan, W. Chen, Z. P. Xu, *Adv. Mater.* **2017**, *29*, 1700373.

[44] F. Wang, Z. Xie, H. Zhang, C.-Y. Liu, Y.-G. Zhang, *Adv. Funct. Mater.* **2011**, *21*, 1027.

[45] Z. Xie, F. Wang, C. Y. Liu, *Adv. Mater.* **2012**, *24*, 1716.

[46] M. Sun, S. Qu, Z. Hao, W. Ji, P. Jing, H. Zhang, L. Zhang, J. Zhao, D. Shen, *Nanoscale* **2014**, *6*, 13076.

[47] C.-C. Shih, P.-C. Chen, G.-L. Lin, C.-W. Wang, H.-T. Chang, *ACS Nano* **2015**, *9*, 312.

[48] Y. Wang, S. Kalytchuk, L. Wang, O. Zhovtiuk, K. Cepe, R. Zboril, A. L. Rogach, *Chem. Commun.* **2015**, *51*, 2950.

[49] J. Liu, N. Wang, Y. Yu, Y. Yan, H. Zhang, J. Li, J. Yu, *Sci. Adv.* **2017**, *3*, 1603171.

[50] Y. Zhao, F. Li, R. Zhang, D. G. Evans, X. Duan, *Chem. Mater.* **2002**, *14*, 4286.

[51] P. Niu, L. Zhang, G. Liu, H. M. Cheng, *Adv. Funct. Mater.* **2012**, *22*, 4763.

[52] P. Niu, L. C. Yin, Y. Q. Yang, G. Liu, H. M. Cheng, *Adv. Mater.* **2014**, *26*, 8046.

[53] Y. Kang, Y. Yang, L. C. Yin, X. Kang, G. Liu, H. M. Cheng, *Adv. Mater.* **2015**, *27*, 4572.

[54] J. Xu, Y. Li, S. Peng, G. Lu, S. Li, *Phys. Chem. Chem. Phys.* **2013**, *15*, 7657.

[55] B. Jürgens, E. Irran, J. Senker, P. Kroll, H. Müller, W. Schnick, *J. Am. Chem. Soc.* **2003**, *125*, 10288.

[56] K. Schwinghammer, M. B. Mesch, V. Duppel, C. Ziegler, J. Senker, B. V. Lotsch, *J. Am. Chem. Soc.* **2014**, *136*, 1730.

[57] M. J. Hudson, S. Carlino, D. C. Apperley, *J. Mater. Chem.* **1995**, *5*, 323.

[58] J. Lee, D. Wong, J. VelascoJr, J. F. Rodriguez-Nieva, S. Kahn, H.-Z. Tsai, T. Taniguchi, K. Watanabe, A. Zettl, F. Wang, L. S. Levitov, M. F. Crommie, *Nat. Phys.* **2016**, *12*, 1032.

[59] W. Liu, S. Xu, Z. Li, R. Liang, M. Wei, D. G. Evans, X. Duan, *Chem. Mater.* **2016**, *28*, 5426.

[60] D. Yan, J. Lu, M. Wei, J. Han, J. Ma, F. Li, D. G. Evans, X. Duan, *Angew. Chem., Int. Ed.* **2009**, *48*, 3073.